9234 *Biochemistry* **2009,** *48,* 9234–9241
DOI: 10.1021/bi9010286

BIOCHEMISTRY
including biophysical chemistry & molecular biology
Article

The Iron−Sulfur Cluster of Pyruvate Formate-Lyase Activating Enzyme in Whole Cells: Cluster Interconversion and a Valence-Localized $[4Fe\text{-}4S]^{2+}$ State†

Jian Yang,‡ Sunil G. Naik,§ Danilo O. Ortillo,§ Ricardo García-Serres,§,⊥ Meng Li,‡ William E. Broderick,∥ Boi Hanh Huynh,*,§ and Joan B. Broderick*,∥

∥*Department of Chemistry and Biochemistry, Montana State University, Bozeman, Montana 59718,* ‡*Department of Chemistry, Michigan State University, East Lansing, Michigan 48824, and* §*Department of Physics, Emory University, Atlanta, Georgia 30322*
⊥*Current address: CEA/iRTSV/LCBM, 17 rue des Martyrs, 38054 Grenoble cx9, France*

Received June 17, 2009; Revised Manuscript Received August 26, 2009

ABSTRACT: Pyruvate formate-lyase activating enzyme (PFL-AE) catalyzes the generation of a catalytically essential glycyl radical on pyruvate formate-lyase (PFL). Purified PFL-AE contains an oxygen-sensitive, labile [4Fe-4S] cluster that undergoes cluster interconversions *in vitro*, with only the $[4Fe\text{-}4S]^{+}$ cluster state being catalytically active. Such cluster interconversions could play a role in regulating the activity of PFL-AE, and thus of PFL, in response to oxygen levels *in vivo*. Here we report a Mössbauer investigation on whole cells overexpressing PFL-AE following incubation under aerobic and/or anaerobic conditions and provide evidence that PFL-AE undergoes cluster interconversions *in vivo*. After 2 h aerobic induction of PFL-AE expression, approximately 44% of the total iron is present in $[4Fe\text{-}4S]^{2+}$ clusters, 6% in $[2Fe\text{-}2S]^{2+}$ clusters, and the remainder as noncluster Fe^{III} (29%) and Fe^{II} (21%) species. Subsequent anaerobic incubation of the culture results in approximately 75% of the total iron being present as $[4Fe\text{-}4S]^{2+}$ clusters, with no detectable $[2Fe\text{-}2S]^{2+}$. Ensuing aerobic incubation of the culture converts the iron species nearly back to the original composition (42% $[4Fe\text{-}4S]^{2+}$, 10% $[2Fe\text{-}2S]^{2+}$, 19% Fe^{III}, and 29% Fe^{II}). The results provide evidence for changes in cluster composition of PFL-AE in response to the redox state of the cell. Furthermore, the Mössbauer spectra reveal that the $[4Fe\text{-}4S]^{2+}$ cluster of PFL-AE in whole cells contains a valence-localized $Fe^{III}Fe^{II}$ pair which has not been previously observed in the purified enzyme. Addition of certain small molecules containing adenosyl moieties, including 5′-deoxyadenosine, AMP, ADP, and methylthioadenosine, to purified PFL-AE reproduces the valence-localized state of the $[4Fe\text{-}4S]^{2+}$ cluster. It is speculated that the $[4Fe\text{-}4S]^{2+}$ cluster of PFL-AE in whole cells may be coordinated by a small molecule, probably AMP, and that such coordination may protect this labile cluster from oxidative damage.

Pyruvate formate-lyase (PFL)[1] is a central metabolic enzyme that catalyzes the first committed step in anaerobic glucose metabolism, and as such it is critical to the survival of facultative anaerobes in low oxygen environments. PFL is expressed under both aerobic and anaerobic conditions, although expression increases 12−15-fold under anaerobic conditions (*1*−*3*). PFL is also regulated posttranslationally, as it undergoes an activation reaction in which the pyruvate formate-lyase activating enzyme generates a catalytically essential glycyl radical at G734 of PFL (*4*, *5*). PFL is the prototypical member of a growing family of glycyl radical enzymes which catalyze reactions such as ribonucleotide reduction, synthesis of benzylsuccinate, and dehydration of glycerol; all of these glycyl radical enzymes are posttranslationally activated by a corresponding activating enzyme, although few of these have been characterized in any detail (*6*).

The pyruvate formate-lyase activating enzyme (PFL-AE) belongs to the radical *S*-adenosylmethionine (SAM) superfamily of enzymes (*7*) and contains a highly conserved CX_3CX_2C motif that is used to coordinate three irons of the catalytically essential [4Fe-4S] cluster (*8*, *9*). The fourth iron of the cluster is coordinated by the carboxyl and amino groups of SAM, as first demonstrated by ENDOR and Mössbauer spectroscopic studies and more recently confirmed by X-ray crystallography (*10*−*13*). ENDOR spectroscopy also revealed the presence of orbital overlap between the sulfonium of SAM and the iron−sulfur cluster (*14*). This orbital overlap, together with the observation that the reduced $[4Fe\text{-}4S]^{+}$ state of PFL-AE is catalytically active and provides the electron required for reductive cleavage of SAM (*15*), suggests a mechanism for activation of PFL in which the initial step is inner-sphere electron transfer from the $[4Fe\text{-}4S]^{+}$ cluster to SAM (*12*). Electron transfer to SAM would then promote cleavage of the S−C5′ bond of SAM to yield a 5′-deoxyadenosyl radical intermediate, which would then abstract a pro-*S* hydrogen from the PFL-G734 residue to produce the catalytically essential glycyl radical.

The PFL glycyl radical is very stable under strict anaerobic conditions ($t_{1/2} > 24$ h) (*12*). Exposure to oxygen, however, results

†This work was supported by grants from the National Institutes of Health (GM54608 to J.B.B. and GM47295 to B.H.H.)

*Corresponding authors. J.B.B.: e-mail, jbroderick@chemistry.montana.edu; phone, (406) 994-6160; fax, (406) 994-5407. B.H.H.: e-mail, vhuynh@emory.edu; phone, (404) 727-4295; fax, (404) 727-0873.

[1]Abbreviations: SAM, *S*-adenosylmethionine; PFL, pyruvate formate-lyase; PFL-AE, pyruvate formate-lyase activating enzyme; LOC, valence-localized; DELOC, valence-delocalized; ENDOR, electron-nuclear double resonance; CoA, coenzyme A; AMP, adenosine 5′-monophosphate; ADP, adenosine 5′-diphosphate; ATP, adenosine 5′-triphosphate; MTA, methylthioadenosine.

 Published on Web 08/27/2009

in rapid and complete cleavage of the PFL protein backbone at the site of the radical (*4*, *5*). The oxygen sensitivity of the PFL glycyl radical is consistent with its role in *anaerobic* glucose metabolism and with the observation that it becomes activated *in vivo* only under anaerobic growth conditions (*16*). The PFL activating enzyme, however, is constitutively expressed under both aerobic and anaerobic conditions (*8*, *17*), which raises questions as to why PFL is activated only under anaerobic conditions and, more specifically, what regulates the activity of the activating enzyme in response to oxygen levels. At one level, our current understanding of the PFL-AE-catalyzed reaction provides insight, as generation of the catalytically active [4Fe-4S]$^{+}$ cluster of PFL-AE requires reduced flavodoxin, which would be more abundant in anaerobic cells (*18*). We have also found, however, that the cluster in PFL-AE is quite labile *in vitro*, with [2Fe-2S] and [3Fe-4S] clusters being observed in addition to [4Fe-4S] clusters, when conditions are not kept sufficiently anaerobic and reducing (*19*−*21*). Further, we observed facile interconversion between the [3Fe-4S] and [4Fe-4S] states of the cluster *in vitro* (*10*, *21*). Our observations led us to question what was the resting state of the PFL-AE iron−sulfur cluster under aerobic conditions *in vivo* and whether cluster interconversions occurred *in vivo* in response to changes in growth conditions.

This paper reports a Mössbauer study of homologously overexpressed recombinant *Escherichia coli* PFL-AE in whole cells. The objectives were to determine the cluster composition of PFL-AE in the cell under different conditions with the intention of identifying possible physiological relevance for the various forms of Fe−S clusters detected in previous *in vitro* studies. Mössbauer spectroscopy was chosen for this study because it can detect, quantify, and distinguish all forms of iron−sulfur clusters and has been successfully applied to characterize the cluster states of both FNR (*22*) and BioB (*23*, *24*) in whole cells. Our results indicate that PFL-AE can undergo cluster interconversions in whole cells in response to growth conditions and that the [4Fe-4S] cluster in PFL-AE *in vivo* exhibits an unusual valence-localized electronic structure.

MATERIALS AND METHODS

Materials. All chemicals and other materials were obtained from commercial sources and were of the highest purity commercially available, unless indicated otherwise.

Construction of PFL-AE Expression and Control Vectors. The pCAL-n-EK/*pflA* vector (hereafter designated pTHVI47) was constructed as previously described (*20*). For construction of the control vector, pTHVI47 was digested with *Nde*I and *Hin*dIII. The fragments were separated on an agarose gel, and the large fragment was purified using a Compass DNA purification kit (American Bioanalytical). The ends were trimmed by using the end conversion mix from the PETBlue-1 perfectly blunt cloning kit (EMD Biosciences); following end conversion the blunt fragment was ligated to generate the control plasmid containing no *pflA* gene. The control plasmid was verified by DNA fingerprinting using *Eco*RV and *Xba*I, as well as by DNA sequencing, and was designated pJYVI119.

Growth, Induction, and Cycling of PFL-AE and Control Cultures. The vectors pTHVI47 and pJYVI119 were transformed into BL21(DE3)pLysS single competent cells to generate PFL-AE expressing and control cells, respectively. Both PFL-AE-expressing and control cells were grown overnight in LB at 37 °C with shaking, and 5 mL of these overnight cultures was used to inoculate 1 L of defined minimal medium enriched with ^{57}Fe (as previously described (*21*)) in a 2800 mL Fernbach flask. The PFL-AE and control cultures were grown with shaking (250 rpm) at 37 °C to an $OD_{600} \sim 0.7$. At this point, IPTG was added to both cultures to a final concentration of 1 mM. The cultures were grown for an additional 2 h under aerobic conditions with shaking. Both cultures were then transferred to a 4 °C cold box and made anaerobic by bubbling N_2 gas through for 16 h. To make the culture aerobic again, air was bubbled through the culture for 6 h. At specific time points after induction, or after transition from aerobic to anaerobic or anaerobic to aerobic conditions, aliquots (60 mL) were removed for the preparation of samples for Mössbauer analysis.

Preparation of Whole-Cell Mössbauer Samples. The aliquots taken during cycling between aerobic and anaerobic conditions were centrifuged to collect cell paste (~0.8 g per 60 mL aliquot). The cell pastes were resuspended in 200 mL of wash solution (50 mM NaCl, 40 mM MOPS, and 22.2 mM glucose) and then centrifuged to collect the cell paste, which was transferred to Mössbauer cups and frozen in liquid nitrogen.

Preparation of Mössbauer Samples of Purified PFL-AE. ^{57}Fe-labeled PFL-AE was purified as previously described (*20*) from cells grown in ^{57}Fe-enriched medium (*21*). In order to investigate the effects of small molecules on the state of the [4Fe-4S]$^{2+}$ cluster, Mössbauer samples were prepared in which the purified [^{57}Fe]-PFL-AE (0.64 mM) was mixed with (in separate samples) ATP, ADP, AMP, 5′-deoxyadenosine, methylthioadenosine, adenine, ribose, pyruvate, formate, CoA, or acetyl-CoA (all at 6.4 mM final concentration). The samples were frozen in liquid nitrogen immediately after mixing. After the Mössbauer spectra were collected, the samples were thawed, and SAM was added to each (to 6.4 mM final concentration). This concentration of SAM was chosen due to the high concentration of protein (0.64 mM) and small molecule (6.4 mM) already in the sample. The samples were flash-frozen for collection of additional Mössbauer data.

Mössbauer Spectroscopy. Mössbauer spectra were recorded in either a weak-field spectrometer equipped with a Janis 8DT variable-temperature cryostat or a strong-field spectrometer furnished with a Janis CNDT/SC SuperVaritemp cryostat encasing an 8 T superconducting magnet. Both spectrometers operate in a constant acceleration mode in a transmission geometry. The zero velocity of the spectra refers to the centroid of a room temperature spectrum of a metallic iron foil.

RESULTS

Construction of PFL-AE-Overexpressing and Control Cells. The PFL-AE expression vector was constructed as previously described (*20*) and, when transformed into *E. coli* BL21-(DE3)pLysS cells, provided a high level of overexpression of PFL-AE (Figure 1). A control vector was constructed by using restriction digestion and ligation to remove the *pflA* gene from the PFL-AE expression vector. This vector, when transformed into the same *E. coli* strain, showed no evidence for overexpression of PFL-AE (Figure 1).

Iron−Sulfur Cluster Interconversions in PFL-AE in Whole Cells. Purified PFL-AE has been previously shown to undergo cluster interconversions. An early report suggested a [2Fe-2S]$^{2+}$ to [4Fe-4S]$^{2+/+}$ interconversion upon reduction of PFL-AE (*19*), while more recent results point to a facile [3Fe-4S]$^{+}$ to [4Fe-4S]$^{2+/+}$ conversion under reducing conditions, with the

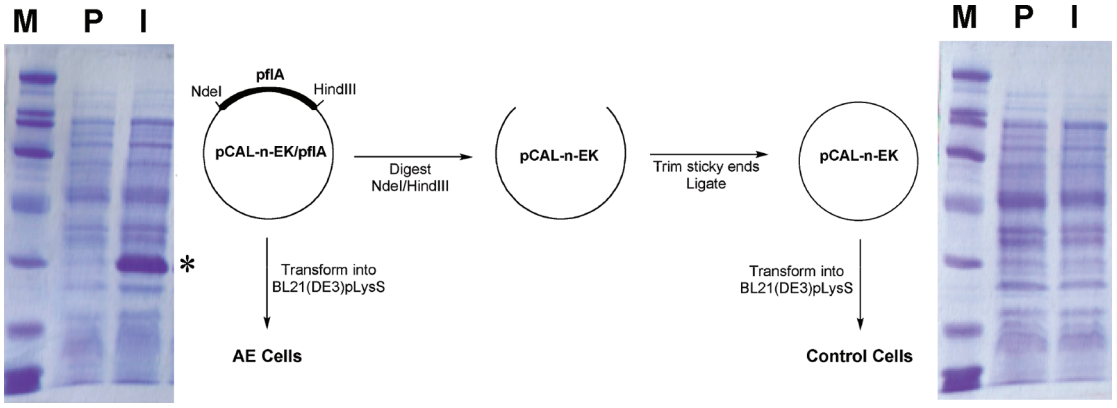

FIGURE 1: Construction of PFL-AE-overexpressing and control cells. The PFL-AE expression vector, constructed as indicated in the figure and described in the text, was transformed into *E. coli* BL21(DE3)pLysS cells. The control vector consisted of the PFL-AE expression vector with the PFL-AE gene removed and was transformed into the same cell line. SDS−PAGE gels showing the results of growth and induction of the PFL-AE (left) and control (right) cells are shown. Lanes on each gel are marked as M (MW standards), P (preinduction), and I (2 h postinduction).

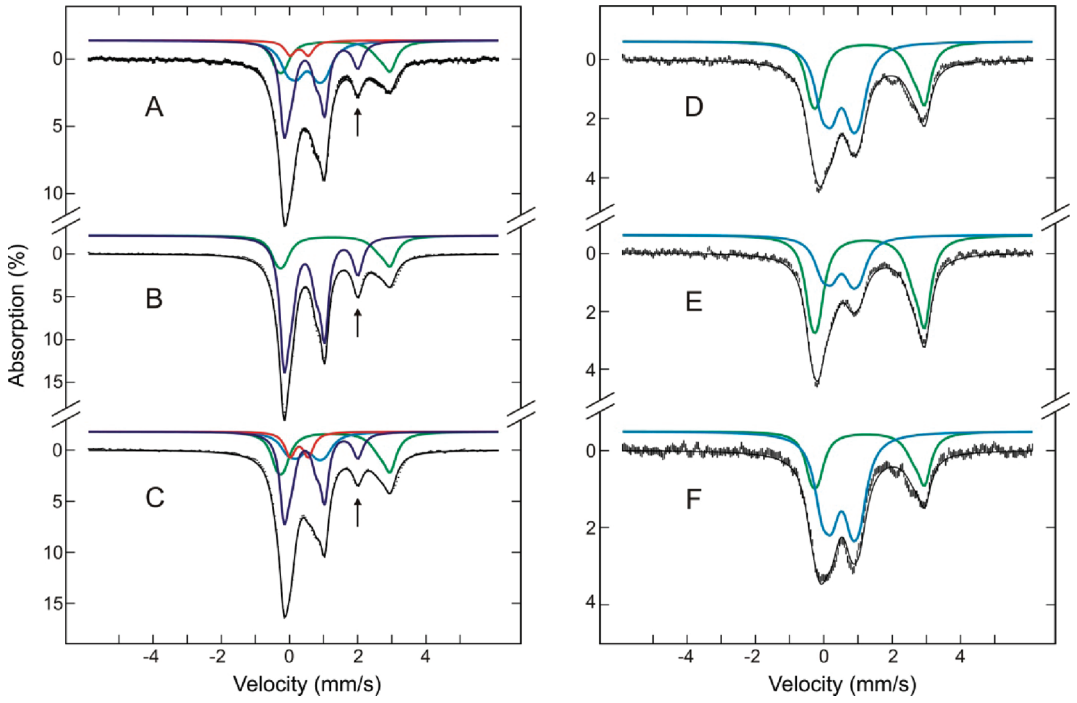

FIGURE 2: Mössbauer spectra of PFL-AE-overexpressing (left panel, A−C) and control (right panel, D−F) cells harvested under different growth conditions: after 2 h induction under aerobic conditions (A and D), followed by 16 h anaerobic incubation (B and E), and further aerobic incubation (C and F). The data (hatched marks) were recorded at 4.2 K in a magnetic field of 50 mT applied parallel to the γ-beam. The colored lines are the theoretical simulations of component spectra that sum to a theoretical spectrum (black solid lines overlaying experimental data) in good agreement with the experimental data. Component spectral simulations are color-coded as red for $[2Fe\text{-}2S]^{2+}$, blue for LOC $[4Fe\text{-}4S]^{2+}$, green for noncluster Fe^{II}, and cyan for noncluster Fe^{III}. Spectral parameters for the LOC $[4Fe\text{-}4S]^{2+}$ are given in the text and list in Table 1. The spectrum of the $[2Fe\text{-}2S]^{2+}$ cluster is simulated with a single quadrupole doublet of $\delta = 0.28$ mm/s and $\Delta E_Q = 0.53$ mm/s. The spectrum of the noncluster Fe^{III} is simulated with two equal intensity quadrupole doublets with $\delta_1 = 0.50$ mm/s, $\Delta E_{Q1} = 1.10$ mm/s and $\delta_2 = 0.52$ mm/s, $\Delta E_{Q2} = 0.57$ mm/s. The spectrum of the noncluster Fe^{II} is simulated with two quadrupole doublets of intensity ratio of 1.4:1 with $\delta = 1.39$ mm/s and $\Delta E_Q = 3.13$ mm/s for the intense doublet and $\delta = 1.13$ mm/s and $\Delta E_Q = 3.01$ mm/s for the other doublet. The signal quantifications are provided in the text.

corresponding $[4Fe\text{-}4S]^{2+/+}$ to $[3Fe\text{-}4S]^{+}$ occurring upon oxidation (*10*, *21*). The physiological relevance of these cluster conversions, if any, has yet to be determined. PFL-AE is constitutively expressed in *E. coli* under both aerobic and anaerobic growth conditions; however, it activates PFL only under anaerobic reducing conditions. Our observations of PFL-AE cluster interconversions *in vitro* led us to question whether cellular redox-state-dependent cluster interconversions might exist and play a role in regulating PFL-AE activity. To address this possibility, we have used Mössbauer spectroscopy to investigate possible PFL-AE cluster interconversions in *E. coli* cells overexpressing PFL-AE under varying air-exposure growth conditions.

After 2 h induction under aerobic conditions, *E. coli* cells overexpressing PFL-AE show a Mössbauer spectrum (Figure 2A) that can be decomposed into four-component spectra. On the basis of their Mössbauer parameters (given in Table 1, caption of Figure 2, and the following paragraph) and magnetic-field-dependent properties, these four-component spectra are attributed to (1) valence-localized $[4Fe\text{-}4S]^{2+}$ clusters (accounting for ~44% of total iron; blue line in Figure 2), (2) $[2Fe\text{-}2S]^{2+}$ clusters (~6% of total iron; red line), (3) high-spin

Table 1: Comparison of Mössbauer Parameters for the $[4Fe\text{-}4S]^{2+}$ Cluster Observed in Whole Cells Expressing PFL-AE and in Purified Enzyme

state	Fe sites	δ (mm/s)	ΔE_Q (mm/s)	η	relative intensity
whole cell	1: DELOC $Fe^{II}Fe^{III}$	0.43	1.20	0.0	2
	2: LOC Fe^{III}	0.43	0.71	0.5	1
	3: LOC Fe^{II}	0.97	2.08	0.7	1
purified PFL-AE	1: DELOC $Fe^{II}Fe^{III}$	0.44	1.20	0.6	2
	2: DELOC $Fe^{II}Fe^{III}$	0.44	0.98	0.7	2
purified PFL-AE + 5′-dAdo, AMP, ADP, or MTA	1: DELOC $Fe^{II}Fe^{III}$	0.44	1.20	0.5	2
	2: LOC Fe^{III}	0.39	0.52	0.5	1
	3: LOC Fe^{II}	1.00	2.07	0.6	1
purified PFL-AE + SAM	1: DELOC $Fe^{II}Fe^{III}$	0.43	1.22		2
	2: Fe^{III}	0.40	0.77		1
	3: unique site	0.71	1.17		1

Fe^{III} species (~29% of total iron; cyan line), and (4) high-spin Fe^{II} species of N, O ligations (~21% of total iron; green line) (Figure 2A). The component spectrum arising from the $[4Fe\text{-}4S]^{2+}$ clusters in whole cells is different from the spectrum of $[4Fe\text{-}4S]^{2+}$ clusters in purified PFL-AE (*21*) and indicates the presence of a valence-localized $Fe^{II}Fe^{III}$ pair in the whole cell cluster. More detailed descriptions on the spectral properties and analysis of this component spectrum will be given below. The latter two components, attributed to Fe^{III} and Fe^{II} species, are commonly observed in whole cell Mössbauer measurements (*24*, *25*) and have been suggested to represent nonspecific Fe stored in the cells. In accord with such a suggestion, the corresponding sample of control *E. coli* cells, which contain the same plasmid for expressing PFL-AE but without the *pflA* gene, cultivated under the same growth conditions, exhibits Mössbauer signals arising only from the Fe^{III} (~60% of total iron) and Fe^{II} (~40% of total iron) species (Figure 2D). Signals arising from Fe-S clusters are not observed in the control cells, thereby providing evidence that the Fe-S cluster signals observed in the PFL-AE cells are due solely to PFL-AE Fe-S clusters.

After 16 h of subsequent anaerobic incubation, the iron speciation of the PFL-AE cells changes dramatically, such that $[4Fe\text{-}4S]^{2+}$ clusters (~75% of total iron) and Fe^{II} species (~25% of total iron) are the only species observed (Figure 2B). Further aerobic incubation resulted in the PFL-AE cells containing again a mixture of all four species in a composition (~42% $[4Fe\text{-}4S]^{2+}$, 10% $[2Fe\text{-}2S]^{2+}$, ~19% Fe^{III}, and ~29% Fe^{II} (Figure 2C)) similar to that of cells cultivated after 2 h aerobic induction. The corresponding control cells show some variation in the relative amount of Fe^{III} and Fe^{II} present, with Fe^{III} decreasing under anaerobic growth conditions (60% to 37% after 16 h anaerobic incubation) and increasing under anaerobic growth conditions (37% to 66% after 30 min aerobic incubation) (Figure 2D−F). It should be noted that the amount of signal attributed to Fe^{II} in the PFL-AE cells changes little in response to the change in oxygen availability, while the amount of the Fe^{III}, $[2Fe\text{-}2S]^{2+}$, and $[4Fe\text{-}4S]^{2+}$ changes significantly. Consequently, the sum of the quantities of iron present in these three signals in aerobic cultures (44% + 6% + 29% of total iron) is approximately equal to the amount of iron in the $[4Fe\text{-}4S]^{2+}$ (75% of total iron) after anaerobic incubation of the culture. This provides support for the hypothesis that, under anaerobic conditions, additional $[4Fe\text{-}4S]^{2+}$ clusters are assembled in PFL-AE at the expense of the $[2Fe\text{-}2S]^{2+}$ clusters and Fe^{III} present under aerobic growth conditions. Together, these results provide evidence for oxygen-dependent cluster interconversions occurring in PFL-AE *in vivo*, with a mixture of $[4Fe\text{-}4S]^{2+}$ and $[2Fe\text{-}2S]^{2+}$ clusters present under aerobic growth conditions, converting to all $[4Fe\text{-}4S]^{2+}$ under anaerobic conditions. Such cluster interconversions are presumably mediated, at least in part, by the iron−sulfur cluster assembly machinery in *E. coli* (the Isc proteins) (*26*) as well as the inherent oxygen lability of the site-differentiated $[4Fe\text{-}4S]^{2+}$ cluster in PFL-AE.

Valence-Localized $[4Fe\text{-}4S]^{2+}$ in PFL-AE in Whole Cells. A surprising discovery made in the current study is that the Mössbauer spectral features of the $[4Fe\text{-}4S]^{2+}$ cluster of PFL-AE in whole cells are distinct from those previously reported for the purified protein. The $[4Fe\text{-}4S]^{2+}$ cluster of the purified protein exhibits a Mössbauer spectrum that can be decomposed into two unresolved equal-intensity quadrupole doublets with parameters ($\delta_1 = 0.45$ mm/s, $\Delta E_{Q1} = 1.15$ mm/s and $\delta_2 = 0.45$ mm/s, $\Delta E_{Q2} = 1.00$ mm/s) that are indicative of valence-delocalized (DELOC) $Fe^{II}Fe^{III}$ pairs (*21*), as commonly observed for $[4Fe\text{-}4S]^{2+}$ clusters (*27*). The $[4Fe\text{-}4S]^{2+}$ cluster in PFL-AE in whole cells, however, contains a valence-localized (LOC) $Fe^{II}Fe^{III}$ pair, as indicated by the prominent peak at approximate +1.9 mm/s (Figure 2A, arrows; also see Figure 3A); this peak is the high-energy peak of a quadrupole doublet (Figure 3A, magenta line) with parameters ($\delta = 0.97$ mm/s and $\Delta E_Q = 2.08$ mm/s) that are indicative of high-spin Fe^{II}. The magnetic field dependence of this doublet demonstrates that it arises from a diamagnetic ($S = 0$) state (Figure 3B). The corresponding Fe site, therefore, cannot be attributed to a monomeric high-spin ($S = 2$) Fe^{II} species and must be part of a diamagnetic Fe cluster. This site is thus assigned to the Fe^{II} site (designated Fe site 3) of a LOC $Fe^{II}Fe^{III}$ pair in the diamagnetic $[4Fe\text{-}4S]^{2+}$ cluster. In addition, two other quadrupole doublets are observed to arise from the $[4Fe\text{-}4S]^{2+}$ cluster of PFL-AE in whole cells (Figure 3A). One quadrupole doublet (Figure 3A, purple line), designated to Fe site 1, exhibits absorption intensity twice as intense as that of Fe site 3 and has parameters ($\delta = 0.43$ mm/s and $\Delta E_Q = 1.20$ mm/s) consistent with a DELOC $Fe^{II}Fe^{III}$ pair in a $[4Fe\text{-}4S]^{2+}$ cluster. The other doublet ($\delta = 0.43$ mm/s and $\Delta E_Q = 0.71$ mm/s) (Figure 3A, cyan line) has an intensity similar to that of Fe site 3. On the basis of its intensity and Mössbauer parameters, we assign this doublet to the Fe^{III} site (designated as Fe site 2) of the LOC pair. A spectrum recorded at 6 T (Figure 3B) indicates that these latter two quadrupole doublets are also arising from a diamagnetic system, consistent with their assignment as Fe sites in a diamagnetic $[4Fe\text{-}4S]^{2+}$ cluster. The relative signal intensity of the three quadrupole doublets, mentioned above (2:1:1 for site 1:site 2:site 3), not only supports their assignment as the DELOC pair and the two LOC sites, respectively, but also suggests that 100% of the $[4Fe\text{-}4S]^{2+}$ clusters in PFL-AE in whole cells are in this LOC state.

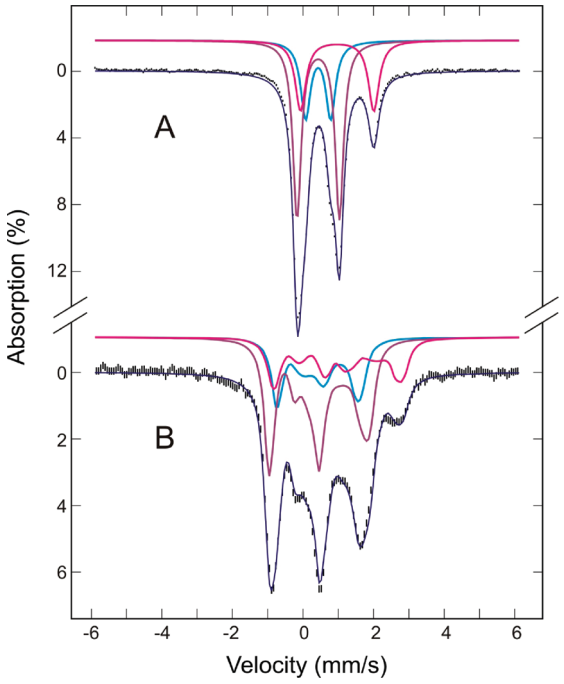

FIGURE 3: Mössbauer spectra of the LOC $[4Fe\text{-}4S]^{2+}$ cluster of PFL-AE in whole cells. The data (hatched marks) were recorded at 4.2 K in a parallel applied field of (A) 50 mT or (B) 6 T. These spectra were prepared by removing the noncluster Fe^{II} contribution (26%) from the raw data of the 16 h anaerobic growth cells (see Figures 2B and S3). The solid lines displayed above the experimental spectra are theoretical simulations of the component spectra, which are color-coded as purple for the DELOC $Fe^{II}Fe^{III}$ pair (site 1), cyan for the Fe^{III} site (site 2), and magenta for the LOC Fe^{II} unique site (site 3). The blue lines overlaid with the data are the composite spectra. The 6 T spectrum is simulated with the assumption of diamagnetism. The excellent agreement between theory and experiment supports the assignment of a diamagnetic $[4Fe\text{-}4S]^{2+}$ cluster.

Previously, we reported that the [4Fe-4S] cluster in purified PFL-AE contains a unique Fe site that binds the cosubstrate SAM in both the $[4Fe\text{-}4S]^{2+}$ and $[4Fe\text{-}4S]^{+}$ states (*8*, *9*). By selectively labeling the unique Fe site with ^{57}Fe, we demonstrated that binding of SAM affects the Mössbauer spectrum of the unique site in the $[4Fe\text{-}4S]^{2+}$ cluster significantly; in the absence of SAM, this unique Fe site gave rise to a Mössbauer spectrum typical for the Fe atoms in a $[4Fe\text{-}4S]^{2+}$ cluster, with $\delta = 0.42$ mm/s and $\Delta E_Q = 1.12$ mm/s. Upon addition of SAM, a substantial increase in the isomer shift ($\delta = 0.72$ mm/s, $\Delta E_Q = 1.15$ mm/s) signaled an increase in coordination number and/or binding of more ionic ligands than sulfur (*10*). Subsequent ENDOR studies provided direct evidence for coordination of SAM to the unique Fe site through binding of the amino and carboxylate groups (*9*). The large isomer shift (0.97 mm/s) and quadrupole splitting (2.08 mm/s) observed for site 3 of the $[4Fe\text{-}4S]^{2+}$ cluster in PFL-AE in whole cells are indicative not only of valence localization at that site but also of an unusual coordination that is atypical for the FeS_4 environment found in [4Fe-4S] clusters; the requirement for unusual coordination implicates the unique Fe site of the $[4Fe\text{-}4S]^{2+}$ cluster, which has the demonstrated ability to exchange ligands, as the LOC Fe^{II} site. The unusually large values of the parameters, however, do not appear to be a result of SAM binding, since SAM bound to purified proteins gives rise to a spectrum of the unique Fe site with different and smaller parameters (see above and Table 1).

Valence-Localized $[4Fe\text{-}4S]^{2+}$ in Purified PFL-AE. In an effort to explore the factors associated with valence localization

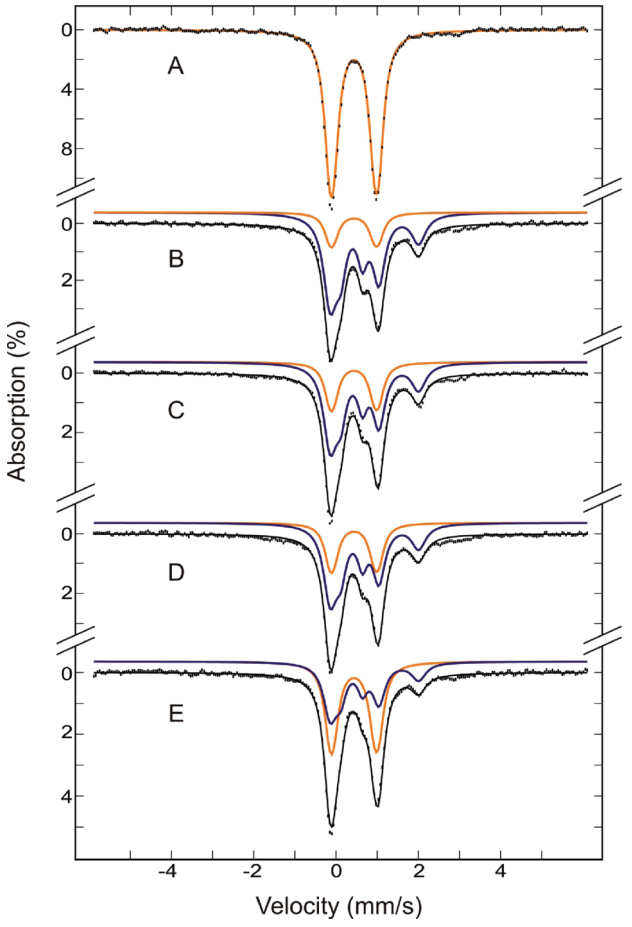

FIGURE 4: Mössbauer spectra of purified PFL-AE (0.64 mM) alone (A) and in the presence of 5′-dAdo (B), AMP (C), MTA (D), or ADP (E) (6.4 mM each). The spectra (hatched marks) were recorded at 4.2 K in a parallel field of 50 mT. The solid lines are theoretical spectra simulated with parameters quoted in the text. They are color coded for the "unbound" DELOC $[4Fe\text{-}4S]^{2+}$ cluster in the purified PFL-AE (orange) and for the "bound" LOC $[4Fe\text{-}4S]^{2+}$ (blue). The fraction of LOC cluster is at a maximum of 77% of total Fe in the presence of 5′-dAdo and decreases to 69%, 65%, and 50% in the presence of AMP, MTA, and ADP, respectively. The small absorption peak at ~3.0 mm/s indicates the purified enzyme contains ~5% Fe^{II} impurity.

in the $[4Fe\text{-}4S]^{2+}$ cluster, Mössbauer spectra were obtained for purified PFL-AE in the presence of a series of small molecules, including potential SAM degradation products (methylthioadenosine, 5′-deoxyadenosine, methionine, adenine, and ribose), substrates and products of PFL (pyruvate, formate, CoA, and acetyl-CoA), and abundant cellular metabolites (ATP, ADP, and AMP). The LOC state was produced by addition of methylthioadenosine, 5′-deoxyadenosine, AMP, or ADP to PFL-AE, as evidenced by the appearance of a prominent peak in the Mössbauer spectra at approximate +1.9 mm/s (Figure 4). For comparison, the Mössbauer spectrum of PFL-AE purified from anaerobically grown cells is also shown in Figure 4. In contrast to PFL-AE purified from aerobically grown cells, which contains a mixture of various types of Fe-S clusters (*21*), PFL-AE purified from anaerobically grown cells contains only $[4Fe\text{-}4S]^{2+}$ cluster and a trace amount of Fe^{II} impurity (~5% of total Fe). As expected for a typical $[4Fe\text{-}4S]^{2+}$ cluster, the Mössbauer spectrum of the purified enzyme (Figure 4A) can be fitted with two unresolved equal-intensity quadrupole doublets with parameters ($\delta_1 = 0.44$ mm/s, $\Delta E_{Q1} = 1.20$ mm/s and $\delta_2 = 0.44$ mm/s,

ΔE_{Q2} = 0.98 mm/s) that are consistent with DELOC $Fe^{II}Fe^{III}$ pairs. Detailed analysis of the spectrum of purified PFL-AE in the presence of 5′-deoxyadenosine, AMP, methylthioadenosine, or ADP (Figure 4B−E) indicates that all four spectra can be decomposed into two-component spectra. The one-component spectrum is identical to that of the purified enzyme (orange line). The other component is a spectrum (blue line) consisting of three distinct quadrupole doublets (δ_1 = 0.44 mm/s, ΔE_{Q1} = 1.20 mm/s; δ_2 = 0.39 mm/s, ΔE_{Q2} = 0.52 mm/s; and δ_3 = 1.00, ΔE_{Q3} = 2.07 mm/s) in a 2:1:1 ratio of relative intensities. The latter component spectrum is very similar to the spectrum of the $[4Fe\text{-}4S]^{2+}$ cluster in whole cells, and accordingly, the three doublets with intensity ratio of 2:1:1 are assigned to a DELOC $Fe^{II}Fe^{III}$ pair, a LOC Fe^{III}, and a LOC Fe^{II} (the unique iron site) site, respectively. High-field studies show that both components are arising from diamagnetic systems (Supporting Information Figure S1), consistent with the assigned "typical" $[4Fe\text{-}4S]^{2+}$ (orange) and LOC $[4Fe\text{-}4S]^{2+}$ (blue) states. The observation of the former spectral component indicates a portion of the clusters in each sample is in the resting unbound state. The fraction of clusters in the LOC-bound state varied with the identity of the small molecule and in no case was 100%. The remaining molecules examined for the ability to produce the LOC state had no significant impact on the Mössbauer spectrum of PFL-AE (Supporting Information Figure S2). It is concluded that these molecules either do not bind PFL-AE or do not bind in such a way as to perturb the $[4Fe\text{-}4S]^{2+}$ cluster. A common structural unit for the coordinated molecules is the adenosyl group, and the fraction of bound clusters appears to decrease with increasing size of the molecule involved (Figure 4), such that binding of ATP, CoA, or acetyl-CoA is excluded. This is not surprising as the size of bound molecule may be limited by accessibility to and/or dimension of the binding pocket.

Together, these results demonstrate that the LOC $[4Fe\text{-}4S]^{2+}$ state observed for PFL-AE in whole cells can be reproduced in the purified protein by addition of certain adenosyl-containing molecules, including ADP, AMP, 5′-dAdo, and MTA. The appearance of a LOC site with a large isomer shift of 0.97 mm/s can best be explained by a change in coordination of the unique site of the $[4Fe\text{-}4S]^{2+}$ of PFL-AE upon addition of these molecules. Whether the adenosyl moieties coordinate to the unique site, or whether their binding in a proximal pocket somehow changes the coordination of the unique site, remains to be determined. Regardless of the mechanism by which the valence localization occurs, it seems likely that an abundant intracellular molecule containing an adenosyl moiety is responsible for the valence localization observed in PFL-AE in whole cells. Of the molecules that cause valence localization in the purified protein, only AMP would be considered to be abundant in *E. coli* cells, and thus we consider AMP the most likely candidate for binding to PFL-AE in whole cells and generating the LOC state.

Displacement of Bound Molecules by the Cosubstrate SAM. To investigate whether the cosubstrate SAM has the ability to displace the small molecules bound to the $[4Fe\text{-}4S]^{2+}$ clusters in PFL-AE, SAM was added to the samples containing 5′-dAdo- and ADP-bound PFL-AE; these samples were chosen for SAM addition because they represented the greatest (5′-dAdo) and least (ADP) degree of valence localization. As a reference, SAM was also added to purified enzymes in the absence of small molecules. After SAM addition, all three samples exhibit spectra that are, for all intents and purposes, indistinguishable (Figure 5). These spectra can be simulated with

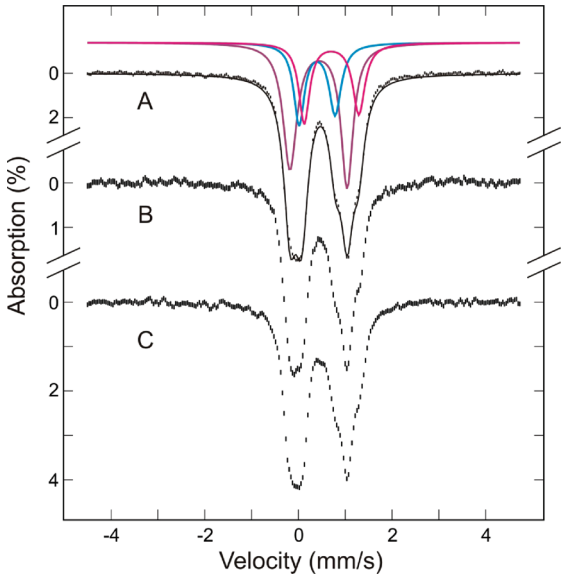

FIGURE 5: Mössbauer spectra of purified PFL-AE (0.64 mM) in the presence of cluster-bound small molecules and/or SAM (6.4 mM): (A) purified PFL-AE with SAM, (B) purified PFL-AE with 5′-dAdo plus SAM, and (C) purified PFL-AE with ADP plus SAM. The data (hatched marks) were recorded at 4.2 K in a parallel field of 50 mT. For clarity, contributions (~4% of total Fe) from the Fe^{II} impurity (see Figure 4) have been removed from the raw data. The latter two spectra (B and C) are practically identical to spectrum A of the SAM-bound $[4Fe\text{-}4S]^{2+}$ cluster, indicating that SAM displaces other bound small molecules. The solid blue line overlaid with spectrum A is the theoretical simulation for the SAM bound cluster, using the parameters quoted in the text (and listed in Table 1). The component spectra are shown above spectrum A and are color-coded for the DELOC $Fe^{II}Fe^{III}$ pair (purple), the Fe^{III} site (cyan), and the SAM-bound unique Fe site (magenta).

three overlapping quadrupole doublets with a relative intensity ratio of 2:1:1, representing the DELOC $Fe^{II}Fe^{III}$ pair (site 1, δ = 0.43 mm/s, ΔE_Q = 1.22 mm/s), the Fe^{III} site (site 2, δ = 0.40 mm/s, ΔE_Q = 0.77 mm/s), and the unique Fe site (site 3, δ = 0.71 mm/s, ΔE_Q = 1.17 mm/s), respectively. Within experimental errors, the parameters obtained for the unique Fe site are identical to those determined for the SAM-bound, selectively labeled ^{57}Fe unique site (*10*), providing evidence supporting the displacement of the small molecules by SAM. Further, the relative intensity ratio of 2:1:1 indicates that displacement of the coordinated small molecules by SAM is 100% complete.

DISCUSSION

We have used Mössbauer spectroscopy to investigate the states of the Fe-S clusters in homologously overexpressed recombinant *E. coli* PFL-AE in whole cells. The results provide evidence for reversible $[2Fe\text{-}2S]^{2+}$ to $[4Fe\text{-}4S]^{2+}$ cluster interconversion occurring in PFL-AE in growing *E. coli* cells; although the results presented here are for cells with very high PFL-AE expression levels (as was necessary to obtain Mössbauer spectra), it is reasonable to expect that similar cluster interconversions occur under truly "native" conditions. Air exposure degrades some of the $[4Fe\text{-}4S]^{2+}$ clusters into $[2Fe\text{-}2S]^{2+}$ clusters with a concomitant appearance of Fe^{III} species as the other products of cluster degradation. Prolonged anaerobic incubation of the air-exposed cells converts *all* of the $[2Fe\text{-}2S]^{2+}$ clusters and Fe^{III} products back to $[4Fe\text{-}4S]^{2+}$ clusters. Similar *in vivo* cluster interconversions were observed for FNR overexpressed in *E. coli* (*22*). In the case of FNR, the $[2Fe\text{-}2S]^{2+}$ to $[4Fe\text{-}4S]^{2+}$ cluster interconversion

is physiologically relevant, with the conversion of [2Fe-2S] to [4Fe-4S] cluster being accompanied by protein dimerization and onset of DNA-binding properties, all triggered by the conversion from aerobic to anaerobic conditions. Such cluster interconversion may also be physiologically relevant for PFL-AE since only the catalytically relevant [4Fe-4S] state is produced under anaerobic culture conditions, conditions under which PFL-AE is expected to be catalytically active. The building of the [4Fe-4S] clusters in PFL-AE upon transition to anaerobic conditions is presumably mediated by the iron−sulfur cluster assembly machinery of *E. coli*, while the degradation to [2Fe-2S] clusters under aerobic conditions may be a result of the oxygen lability of the site-differentiated [4Fe-4S] cluster of PFL-AE.

Our results also provide unequivocal evidence for the presence of an unusual LOC $[4Fe\text{-}4S]^{2+}$ in PFL-AE in whole cells. The cluster present in PFL-AE in whole cells is distinctly different from that in the purified protein, with the latter showing a typical $[4Fe\text{-}4S]^{2+}$ Mössbauer spectrum resulting from two DELOC $Fe^{II}Fe^{III}$ pairs, while the former gives rise to a Mössbauer spectrum indicative of a LOC site in a $[4Fe\text{-}4S]^{2+}$ cluster. The $[4Fe\text{-}4S]^{2+}$ cluster of PFL-AE therefore has unusual properties *in vivo* that are lost upon protein purification, perhaps due to the loss of a small molecule ligand. In general, spectroscopic and structural characterizations of metallocenters in proteins are performed with purified proteins. Our observation, reported here, indicates that such conventional practices may yield information that does not reflect the states of the centers under "native" environments, particularly for centers that are sensitive to environmental conditions, such as the Fe-S cluster of the radical SAM enzymes.

The $[4Fe\text{-}4S]^{2+}$ cluster in PFL-AE in whole cell provides only the second example of valence localization in a protein-bound $[4Fe\text{-}4S]^{2+}$ cluster. The first such example was for the two-electron-reduced ferredoxin thioredoxin reductase (FTR), in which the LOC site is an iron coordinated by a cysteine thiolate and in van der Waals contact with a thiol of the reduced active site disulfide (*28*). The LOC Fe^{II} in FTR has been suggested to play a pivotal role in the enzyme function by anchoring the cluster-interacting thiol in the two-electron-reduced FTR and thereby freeing the other thiol for nucleophilic attack at the disulfide of the substrate thioredoxin (*28*). The cause for the valence localization in PFL-AE in whole cells has not been unequivocally determined, however. Studies presented herein on the purified protein demonstrate that valence localization can be induced by addition of certain small molecules containing adenosyl moieties. Whether one of these small molecules tested might be responsible for the *in vivo* properties of the [4Fe-4S] cluster of PFL-AE has yet to be determined. The level of overexpression of PFL-AE in the *E. coli* cells used in these experiments is estimated to be ~0.5 mM; therefore, a small molecule binding to PFL-AE and causing valence localization would have to be quite abundant, as 100% of the $[4Fe\text{-}4S]^{2+}$ clusters in PFL-AE in whole cells are in the LOC state. Of the molecules causing valence localization in the purified protein, only AMP is expected to be of sufficient abundance in the cell to bind all of the PFL-AE, and thus our current working hypothesis is that AMP binding to PFL-AE is responsible for the unusual cluster properties *in vivo*. The physiological reason for binding of small molecules to PFL-AE in whole cell is not known. We have, however, noticed that the LOC cluster in whole cell appears to be stabilized against oxidative degradation, as 30 min exposure to air resulted in no change in the cluster composition. By comparison, the [4Fe-4S] cluster in purified PFL-AE is rapidly degraded to the [3Fe-4S] and [2Fe-2S] forms upon exposure to air. It is therefore possible that coordination of small molecules to the unique site could be a means to protect the [4Fe-4S] cluster from oxidative damage by preventing the unique Fe site from dissociating from the cluster upon air exposure. Such a protection should not have an adverse effect on the enzyme activity as the bound molecule can be displaced by the cosubstrate SAM. Currently, it is not clear whether such a protection mechanism is commonly employed for anaerobic radical-SAM enzymes. But, the fact that all radical-SAM enzymes of known structure (*10*, *26*−*28*) exhibit similar protein environments surrounding the SAM-bound [4Fe-4S] core suggests strongly that the observed LOC $[4Fe\text{-}4S]^{2+}$ cluster in PFL-AE in whole cells is likely not an isolated event.

ACKNOWLEDGMENT

The authors thank Kaitlin Duschene for assistance in preparation of the Table of Contents illustration.

SUPPORTING INFORMATION AVAILABLE

Mössbauer spectra of purified PFL-AE in the presence of metabolites; 6 T Mössbauer spectrum of purified PFL-AE in the presence of 5′-dAdo; 6 T Mössbauer spectrum of 16 h anaerobic growth cells. This material is available free of charge via the Internet at http://pubs.acs.org.

REFERENCES

1. Sawers, G., and Bock, A. (1988) Anaerobic regulation of pyruvate formate-lyase from *Escherichia coli* K12. *J. Bacteriol. 170*, 5330–5336.
2. Sawers, G., and Bock, A. (1989) Novel transcriptional control of the pyruvate formate-lyase gene: upstream regulatory sequences and multiple promoters regulate anaerobic expression. *J. Bacteriol. 171*, 2485–2498.
3. Sawers, G., and Summpann, B. (1992) Anaerobic induction of pyruvate formate-lyase gene expression is mediated by the ArcA and FNR proteins. *J. Bacteriol. 174*, 3474–3478.
4. Knappe, J., Neugebauer, F. A., Blaschkowski, H. P., and Gänzler, M. (1984) Post-translational activation introduces a free radical into pyruvate formate-lyase. *Proc. Natl. Acad. Sci U.S.A. 81*, 1332–1335.
5. Wagner, A. F. V., Frey, M., Neugebauer, F. A., Schäfer, W., and Knappe, J. (1992) The free radical in pyruvate formate-lyase is located on glycine-734. *Proc. Natl. Acad. Sci. U.S.A. 89*, 996–1000.
6. Buckel, W., and Golding, B. T. (2006) Radical enzymes in anaerobes. *Annu. Rev. Microbiol. 60*, 27–49.
7. Sofia, H. J., Chen, G., Hetzler, B. G., Reyes-Spindola, J. F., and Miller, N. E. (2001) Radical SAM, a novel protein superfamily linking unresolved steps in familiar biosynthetic pathways with radical mechanisms: functional characterization using new analysis and information visualization methods. *Nucleic Acids Res. 29*, 1097–1106.
8. Rödel, W., Plaga, W., Frank, R., and Knappe, J. (1988) Primary structures of *Escherichia coli* pyruvate formate-lyase and pyruvate formate-lyase-activating enzyme deduced from the DNA nucleotide sequences. *Eur. J. Biochem. 177*, 153–158.
9. Külzer, R., Pils, T., Kappl, R., Hüttermann, J., and Knappe, J. (1998) Reconstitution and characterization of the polynuclear iron-sulfur cluster in pyruvate formate-lyase-activating enzyme. Molecular properties of the holoenzyme form. *J. Biol. Chem. 273*, 4897–4903.
10. Krebs, C., Broderick, W. E., Henshaw, T. F., Broderick, J. B., and Huynh, B. H. (2002) Coordination of adenosylmethionine to a unique iron site of the [4Fe-4S] of pyruvate formate-lyase activating enzyme: A Mössbauer spectroscopic study. *J. Am. Chem. Soc. 124*, 912–913.
11. Walsby, C. J., Ortillo, D., Broderick, W. E., Broderick, J. B., and Hoffman, B. M. (2002) An anchoring role for FeS Clusters: Chelation of the amino acid moiety of S-adenosylmethionine to the unique iron site of the [4Fe-4S] cluster of pyruvate formate-lyase activating enzyme. *J. Am. Chem. Soc. 124*, 11270–11271.
12. Walsby, C., Ortillo, D., Yang, J., Nnyepi, M., Broderick, W. E., Hoffman, B. M., and Broderick, J. B. (2005) Spectroscopic approaches to elucidating novel iron-sulfur chemistry in the "Radical SAM" protein superfamily. *Inorg. Chem. 44*, 727–741.

13. Vey, J. L., Yang, J., Li, M., Broderick, W. E., Broderick, J. B., and Drennan, C. L. (2008) Structural basis for glycyl radical formation by pyruvate formate-lyase activating enzyme. *Proc. Natl. Acad. Sci. U.S. A. 105*, 16137–16141.
14. Walsby, C. J., Hong, W., Broderick, W. E., Cheek, J., Ortillo, D., Broderick, J. B., and Hoffman, B. M. (2002) Electron-nuclear double resonance spectroscopic evidence that S-adenosylmethionine binds in contact with the catalytically active $[4Fe\text{-}4S]^{+}$ cluster of pyruvate formate-lyase activating enzyme. *J. Am. Chem. Soc. 124*, 3143–3151.
15. Henshaw, T. F., Cheek, J., and Broderick, J. B. (2000) The $[4Fe\text{-}4S]^{+}$ cluster of pyruvate formate-lyase activating enzyme generates the glycyl radical on pyruvate formate-lyase: EPR-detected single turnover. *J. Am. Chem. Soc. 122*, 8331–8332.
16. Knappe, J., and Sawers, G. (1990) A radical-chemical route to acetyl-CoA: the anaerobically induced pyruvate formate-lyase system of *Escherichia coli*. *FEMS Microbiol. Rev. 75*, 383–398.
17. Sauter, M., and Sawers, R. G. (1990) Transcriptional analysis of the gene encoding pyruvate formate-lyase-activating enzyme of *Escherichia coli*. *Mol. Microbiol. 4*, 355–363.
18. Knappe, J., Blaschkowski, H. P., Gröbner, P., and Schmitt, T. (1974) Pyruvate formate-lyase of *Escherichia coli*: the acetyl-enzyme intermediate. *Eur. J. Biochem. 50*, 253–263.
19. Broderick, J. B., Duderstadt, R. E., Fernandez, D. C., Wojtuszewski, K., Henshaw, T. F., and Johnson, M. K. (1997) Pyruvate formate-lyase activating enzyme is an iron-sulfur protein. *J. Am. Chem. Soc. 119*, 7396–7397.
20. Broderick, J. B., Henshaw, T. F., Cheek, J., Wojtuszewski, K., Smith, S. R., Trojan, M. R., McGhan, R. M., Kopf, A., Kibbey, M., and Broderick, W. E. (2000) Pyruvate formate-lyase activating enzyme: strictly anaerobic isolation yields active enzyme containing a $[3Fe\text{-}4S]^{+}$ cluster. *Biochem. Biophys. Res. Commun. 269*, 451–456.
21. Krebs, C., Henshaw, T. F., Cheek, J., Huynh, B.-H., and Broderick, J. B. (2000) Conversion of 3Fe-4S to 4Fe-4S clusters in native pyruvate formate lyase activating enzyme: Mössbauer characterization and implications for mechanism. *J. Am. Chem. Soc. 122*, 12497–12506.
22. Popescu, C. V., Bates, D. M., Beinert, H., Münck, E., and Kiley, P. J. (1998) Mössbauer spectroscopy as a tool for the study of activation/inactivation of the transcription regulator FNR in whole cells of *Escherichia coli*. *Proc. Natl. Acad. Sci. U.S.A. 95*, 13431–13435.
23. Benda, R., Bui, B. T. S., Schünemann, V., Florentin, D., Marquet, A., and Trautwein, A. X. (2002) Iron-sulfur clusters of biotin synthase in vivo: a Mössbauer study. *Biochemistry 41*, 15000–15006.
24. Cosper, M. M., Jameson, G. N. L., Eidsness, M. K., Huynh, B. H., and Johnson, M. K. (2002) Recombinant *Escherichia coli* biotin synthase is a $[2Fe\text{-}2S]^{2+}$ protein in whole cells. *FEBS Lett. 529*, 332–336.
25. Matzanke, B. F., Müller, G. I., Bill, E., and Trautwein, A. X. (1989) Iron metabolism of *Escherichia coli* studied by Mössbauer spectroscopy and biochemical methods. *Eur. J. Biochem. 183*, 371–379.
26. Ayala-Castro, C., Saini, A., and Outten, F. W. (2008) Fe-S cluster assembly pathways in bacteria. *Microbiol. Mol. Biol. Rev. 72*, 110–125.
27. Trautwein, A. X., Bill, E., Bominaar, E. L., and Winkler, H. (1991) Iron-containing proteins and related analogs--complementary Mössbauer, EPR, and magnetic susceptibility studies. *Struct. Bonding* (*Berlin*) *78*, 1–95.
28. Walters, E. M., Garcia-Serres, R., Jameson, G. N. L., Glauser, D. A., Bourquin, F., Manieri, W., Schürmann, P., Johnson, M. K., and Huynh, B. H. (2005) Spectroscopic characterization of site-specific $[Fe_4S_4]$ cluster chemistry in ferredoxin:thioredoxin reductase: implications for the catalytic mechanism. *J. Am. Chem. Soc. 127*, 9612–9624.